

Characterization of Ag/Ag₂SO₄ system as reference electrode for *in-situ* electrochemical studies of advanced aqueous supercapacitors

DENYS G GROMADSKYI^{a,b,*}

^aJoint Department of Electrochemical Energy Systems, 38A Vernadsky Ave, 03680 Kyiv, Ukraine

^bNational Technical University of Ukraine “KPI”, 37 Peremohy Ave, 03056, Kyiv, Ukraine

e-mail: d.gromadskyi@gmail.com

MS received 22 December 2015; revised 3 March 2016; accepted 29 March 2016

Abstract. Silver metal covered by Ag₂SO₄ was investigated as a reference electrode for flat three-electrode cells. The potential stability of the Ag/Ag₂SO₄ electrode in neutral aqueous solutions utilized as electrolytes for asymmetric high-voltage supercapacitors is reported. It was found that the potential drift and temperature coefficient of this reference electrode are insignificant. Its use as an alternative to the Ag/AgCl electrode enables one to avoid the contamination of the supporting electrolyte solution by Cl[−] anions, which are oxidized earlier than water molecules and other oxygen-containing anions (SO₄^{2−} or NO₃[−]). Using the data obtained from three-electrode electrochemical measurements with the electrode in question, a graphene–carbon nanotube/MnO₂ supercapacitor cell accumulating 9.8 Wh kg^{−1} of specific energy at 1.75 V was built.

Keywords. Silver sulfate reference electrode; neutral aqueous electrolytes; asymmetric supercapacitor.

1. Introduction

Supercapacitors (or ultracapacitors) are energy storage devices with high specific power¹ widely used in hybrid electric vehicles, customer electronics, etc.^{2,3} Supercapacitor technology is developing extremely fast after the invention of new 3- and 2-dimensional ordered carbons (carbon nanotubes, graphene) serving as electrodes. Furthermore, carbon nanostructures may play the role of a conductive skeleton for redox composites based on transition metal oxides and/or electroconducting polymers.⁴ Recently, most popular among scientists are hybridized systems combining the electrodes with pseudo-capacitance and ‘conventional’ supercapacitor electrodes where capacitance is realized due to the formation of the electric double layer. Such hybrids are known in the literature as asymmetric supercapacitors or supercapatteries.^{5,6}

As a rule, supercapacitor cells are flat ‘sandwich-like’ constructions where both (negatively and positively charged) electrodes are coated onto metallic current collectors and separated by a dielectric film which is permeable for ions of an electrolyte solution. It is noteworthy that the electrodes in the ‘realistic’ supercapacitor have to be situated as close as possible to each other to avoid a decrease/increase in their capacitance/inner resistance,^{7,8} *i.e.*, the distance between

them should be equal to the thickness of a separator (usually several tens of micrometers or less).⁹ Flat design of the cell may also be considered as quasi-all-solid-state because there is no free electrolyte in it (it is fully sorbed by the porous electrodes and separator).

As electrolytes for supercapacitors, aqueous, non-aqueous solutions and room-temperature ionic liquids are employed. Electrolytes based on organic aprotic solvents allow for operating at high voltage (*ca.* 3 V), but their drawbacks are relatively low conductivity, toxicity, flammability and extreme sensitivity to impurities of water.¹⁰ For example, tetrafluoroborates, the most popular salts for commercial devices, are hydrolyzed forming aggressive hydrofluoric acid.^{10–12} ‘Traditional’ H₂O-based systems (solutions of KOH, H₂SO₄) have significantly higher conductivities, although their potential range is lower being limited by the decomposition of water (its theoretical value is 1.23 V).¹⁰ Nevertheless, the use of ‘green’ neutral aqueous solutions (mainly the alkali metal sulfates, nitrates or chlorides) paired with specially selected and mass-balanced electrode materials extends the voltage value up to 2.4 V.^{10,13–15}

In order to fabricate an advanced, mass-balanced, supercapacitor with a maximal potential ‘window’ U_{\max} , the first electrochemical measurements should be performed by means of cyclic voltammetric technique in a three-electrode cell consisting of working, counter and reference electrodes for getting the capacitance

*For correspondence

value C via Eq. 1 and operating potential range of each electrode, as shown in figures 1(a) and (b),

$$C = \frac{I}{v} \quad (1)$$

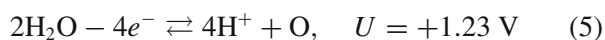
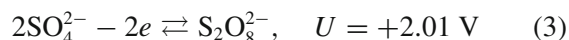
where I is the charge/discharge current (A); v is the scan rate (V s^{-1})

These parameters are interrelated as follows,¹⁴

$$\frac{m_1}{m_2} = \frac{C_2 U_2}{C_1 U_1} \quad (2)$$

where $C_1, C_2; U_1, U_2$ and m_1, m_2 are the capacitances (F); the operating potential ranges (V) and the masses (g), respectively, of the negatively (1) and positively (2) charged electrodes.

It is desirable that the design of this three-electrode cell is similar to that of a supercapacitor device. As a result, this also requires a special, planar design of the reference electrode (RE), since the application of a ‘standard’ glass construction with a salt bridge and Luggin’s capillary¹⁶ is not convenient. In this light, the use of the $\text{Ag}/\text{Ag}_2\text{SO}_4$ system as an RE seems quite logical: SO_4^{2-} anions are electrochemically stable in aqueous solutions because the half-reaction of their oxidation occurs at higher potential U (vs. the normal hydrogen electrode) compared with water. This makes the $\text{Ag}/\text{Ag}_2\text{SO}_4$ system different from Ag/AgCl , where Cl^- anions which play the role of potential-determining ions also have a higher oxidation potential¹⁷ but evolve molecular chlorine earlier than water is decomposed due to the high overpotential of oxygen:



Moreover, the silver sulfate electrode (SSE) is significantly less toxic than the mercury-mercurous sulfate electrode and does not contain of the redox active species like Cu^{2+} cations in the copper-copper sulfate electrode.¹⁸

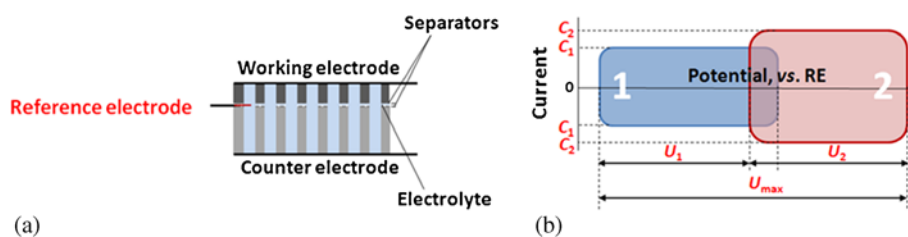


Figure 1. Schematics of, (a) three-electrode supercapacitor cell impregnated with electrolyte solution and (b) cyclic voltammogram of idealized negatively (1) and positively (2) charged supercapacitor electrodes.

It should be noted that the potential of the SSE and its stability strongly depends on the insoluble impurities (mainly AgCl) often contained in the precursors for Ag_2SO_4 producing or forming due to synthetic conditions.¹⁹ According to literature reports,^{19,20} the potential of the $\text{Ag}/\text{Ag}_2\text{SO}_4$ electrode vs. the normal hydrogen electrode varies from +0.34 to +0.71 V.

2. Experimental

Silver sulfate was deposited on the rolled silver wire (Ag , 99.99% trace metal basis) with the geometric sizes of $0.5 \times 5.0 \times 0.05$ mm in the concentrated sulfuric acid (H_2SO_4 , 98%) for 2 h at $+100^\circ\text{C}$ to prevent the inclusion of undesirable impurities into the key compound (Eq. 6):



Then the $\text{Ag}/\text{Ag}_2\text{SO}_4$ sheet was washed in deionized water and dried for 30 min at $+100^\circ\text{C}$ (after that its surface became white-grey).

The freshly prepared SSE was calibrated for 1 h at $+25^\circ\text{C}$ in the glass cell (figure 2) containing 1 mol L^{-1} Na_2SO_4 aqueous solution vs. a commercial silver chloride electrode (BASi RE-5B) with the glass chamber filled with 3 mol L^{-1} KCl aqueous solution at the open circuit potential (OCP) mode.²¹

In addition, OCP was measured immediately after 10 min holding in 1 mol L^{-1} Na_2SO_4 solution at 10, 40 and

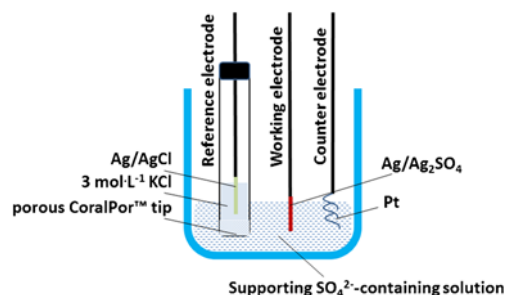


Figure 2. Schematic of glass three-electrode cell for measurements of open circuit potential.

60°C; in 0.1, 0.25, 0.5 and 0.75 mol L⁻¹ Na₂SO₄ solution at +25°C, and in other neutral aqueous electrolytes (NaNO₃, NaCl and KCl with salt concentrations varying from 0.5 to 3 mol L⁻¹) at +25°C. As a source of the potential-determining ions, 0.1 mol L⁻¹ Na₂SO₄ was added to the supporting solution.

The supercapacitor electrodes were studied in flat three- and two-electrode cells. Their electrochemical testing was performed by cyclic voltammetry at the scan rate of 5 mV s⁻¹ via AUT30 potentiostat/galvanostat (Metrohm Autolab, Netherlands). Temperature during electrochemical experiments was of about +25°C.

Working electrodes for the three-electrode cell were made of the (i) raw XGnP[®] graphene nanoplatelets (Grade C, XG Sciences, USA), and (ii) composite based on the purified FloTube[™] multi-walled carbon nanotubes (900, C-Nano, China) and manganese dioxide synthesized by means of a hydrothermal technique from a potassium permanganate precursor as described in Refs.^{22,23} Each electrode besides the active material consisted of a polymer binder (polytetrafluoroethylene, 5 wt%) added in the ethanol media to uniformly disperse their particles. The counter electrode was same as that made of graphene nanoplatelets. Finally, the electrodes were pressed into square pellets (mass loadings 15 mg cm⁻² for working electrode, 65 mg cm⁻² for counter electrode, the geometric surface area was the same for both electrodes) and dried for 4 h at +150°C in a vacuum oven to remove liquid residuals (water, ethanol) sorbed by the porous carbon-based electrodes during manufacturing.

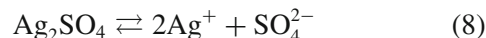
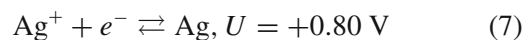
A TF4030 (Nippon Kodoshi, Japan) porous paper film was used as a separator and an extra-buffer for an electrolyte in order to avoid the depletion of the solution near the surface of the working electrode during charge. Titanium foil (Goodfellow Cambridge, UK) played the role of a current collector. All reagents except the graphene nanoplatelets, carbon nanotubes, paper film and titanium foil were obtained from Sigma Aldrich.

The Ag/Ag₂SO₄ RE was situated between two layers of the separator from the edge of the working and counter electrodes, besides these electrodes were rigorously positioned relative to each other to minimize distortions during electrochemical measurements, as has been suggested in Refs.^{24–26}

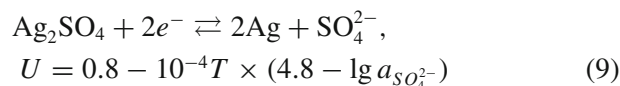
The design of the two-electrode cell was analogous to the three-electrode one and did not contain an RE. Negative (graphene) and positive (carbon nanotube/MnO₂) electrodes were prepared as described above. Their mass loadings were 16.5 and 15 mg cm⁻², respectively, and the thickness was the same in both cases (250±5 μm).

3. Results and Discussion

The Ag/Ag₂SO₄ electrode works as a redox electrode where the corresponding redox reactions between the solid silver and its water insoluble salt take place.¹⁶



The overall reaction can be written as



where T is the temperature (K) and a is activity of the SO₄²⁻ anions (mol L⁻¹) in Nernst's equation.

The stability of the SSE during 1 hour of the OCP measurements is presented in figure 3.

As seen, the potential drift of the investigated electrode is no more than 0.1 mV h⁻¹ with potential deviations of ±0.5 mV evidencing the possibility of its use as an RE in sulfate solutions. Knowing the OCP value of the SSE vs. the silver chloride electrode (*ca.* +0.137 V), it is easy to define its position between other commonly used REs for aqueous solutions²⁷ on the potential scale (figure 4).

Thus, being compared in the hydrogen scale, the Ag/Ag₂SO₄ electrode has the value of OCP in 1 mol L⁻¹ Na₂SO₄ aqueous solution, which is almost identical to that of the copper-copper sulfate electrode in the saturated CuSO₄ aqueous solution (the potential difference is only 20 mV). At the same time, it is interesting that the practical value of OCP for the SSE is lower by about 350 mV than the theoretical one calculated by means of the Nernst equation (Eq. 9). The cause of this deviation may be the impurities of trace metals, such as Zn, Fe, Co, Ni and Hg containing even in the high-purity silver,²⁸ but in order to confirm this assumption a separate detailed study is required which is planned in the near future.

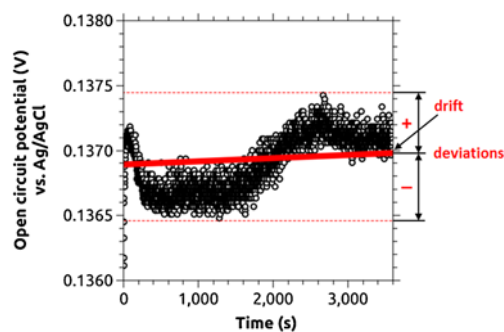


Figure 3. Open circuit potential of silver sulfate electrode in 1 mol L⁻¹ Na₂SO₄ aqueous solution measured at +25°C vs. Ag/AgCl (3 mol L⁻¹ KCl aqueous solution).

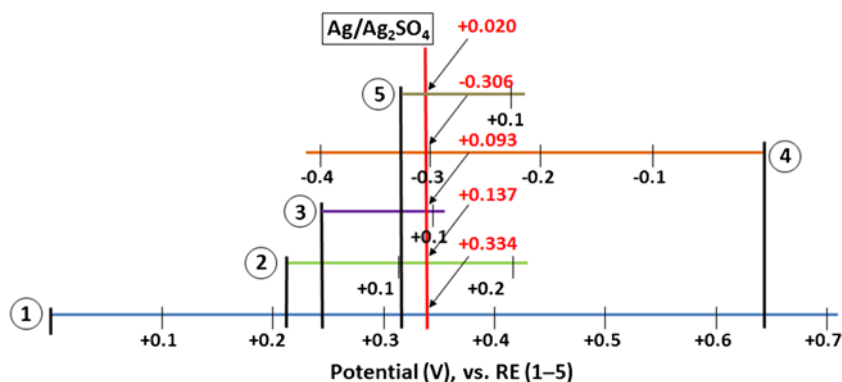


Figure 4. Position of silver sulfate electrode in 1 mol L⁻¹ Na₂SO₄ aqueous solution on the potential scale of different reference electrodes: 1 – normal hydrogen electrode; 2 – silver chloride electrode (3 mol L⁻¹ KCl aqueous solution); 3 – saturated calomel electrode (saturated KCl aqueous solution); 4 – mercury-mercurous sulfate electrode (saturated K₂SO₄ aqueous solution); 5 – copper-copper sulfate electrode (saturated CuSO₄ aqueous solution).

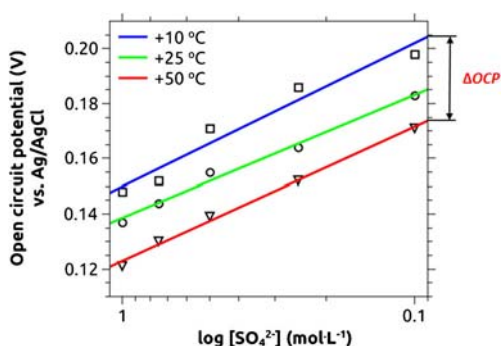


Figure 5. Dependence of open circuit potential for silver sulfate electrode on the concentration of SO₄²⁻ anions in Na₂SO₄ solution at various temperatures.

The temperature behavior of the SSE depending on the concentration of the potential-determining ions is demonstrated in figure 5. It is seen that the OCP of the Ag/Ag₂SO₄ electrode increases with the decrease of the anion concentration in Na₂SO₄ solution for all temperatures studied ($T = +10^{\circ}\text{C}$, $+25^{\circ}\text{C}$ and $+50^{\circ}\text{C}$). It means that the temperature coefficients $\frac{\Delta OCP}{\Delta T}$ are almost similar at the concentration range investigated (0.1–1 mol L⁻¹) and its average value is *ca.* $-0.7 \text{ mV } ^{\circ}\text{C}^{-1}$.

It is valuable to know the influence of third ions (especially Cl⁻) on the potential of the SSE, and the lowest concentration of the potential-determining ions in the supporting electrolyte has been chosen for this purpose (table 1).

The data collected in this table are in good agreement with OCP of the same electrode in pure 0.1 mol L⁻¹ Na₂SO₄ solution (the error between the values obtained is less than $\pm 2\%$), thus showing the potential insensitivity of the Ag/Ag₂SO₄ RE to the cation–anion

Table 1. Values of open circuit potential for silver sulfate electrode in different supporting solutions containing 0.1 mol L⁻¹ Na₂SO₄ vs. Ag/AgCl (in 3 mol L⁻¹ KCl aqueous solution) measured at $+25^{\circ}\text{C}$.

Salt concentration in supporting solution (mol L ⁻¹)	Open circuit potential (V)		
	NaNO ₃ –H ₂ O	NaCl–H ₂ O	KCl–H ₂ O
0.5	0.186	0.185	0.186
1.0	0.183	0.183	0.185
2.0	0.181	0.183	0.183
3.0	0.180	0.181	0.182

composition in the supporting electrolyte where just the concentration of SO₄²⁻ anions plays the key role. This means that the investigated RE is suitable for the majority of neutral aqueous electrolytes. Some problems may arise if the SSE is placed in strong acidic/alkaline solutions through the dissolution of silver sulfate and formation of new insoluble substances (*e.g.*, AgCl in HCl or Ag₂O in KOH), hence an additional calibration of the RE is required.

The electrochemical behaviour of the carbon-based electrodes under applied potential difference vs. Ag/Ag₂SO₄ RE in a ‘model’ electrolyte (1 mol L⁻¹ Na₂SO₄ aqueous solution) is presented in figure 6(a). As seen, the shape of these voltammetric curves is typical for electrodes with electric double layer capacitance (blue line) and pseudo-capacitance (red line): it is almost rectangular for the graphene electrode and contains a few broad intercalation-deintercalation peaks for the carbon nanotube electrode covered with manganese dioxide. Moreover, the positions of the peaks observed in the carbon nanotube/MnO₂ electrode say the predominance of the birnessite phase and the value of specific capacitance of the synthesized composite is

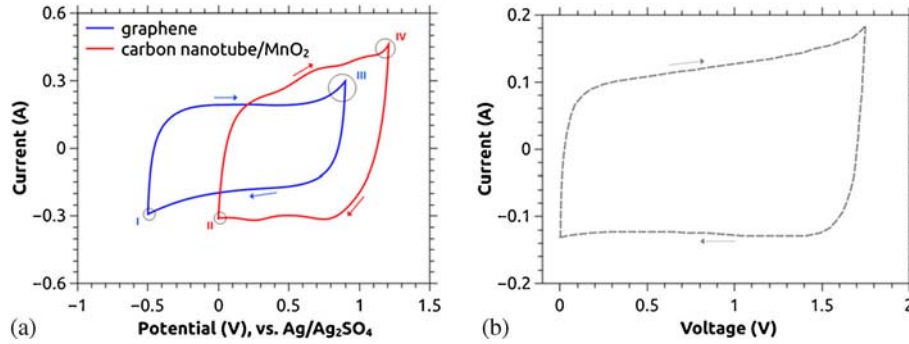


Figure 6. Cyclic voltammograms of, (a) electrodes based on graphene nanoplatelets and carbon nanotube/MnO₂ composite, and (b) mass-balanced asymmetric graphene-carbon nanotube/MnO₂ supercapacitor cell recorded in 1 mol L⁻¹ Na₂SO₄ aqueous solution at +25°C and 5 mV s⁻¹.

Table 2. Some characteristics of graphene and carbon nanotube/MnO₂ electrodes and asymmetrical supercapacitor based on them.

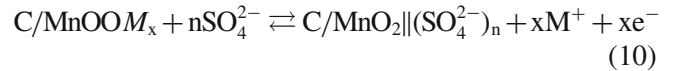
Cell configuration	Parameter	
	Specific capacitance (F g ⁻¹)	Potential range (V)
Ag/Ag ₂ SO ₄ –graphene–counter electrode	88	1.40
counter electrode–carbon nanotube/MnO ₂ –Ag/Ag ₂ SO ₄	114	1.20
graphene–carbon nanotube/MnO ₂	23	1.75

close to that in Ref.²⁹ if only the weight percent of manganese dioxide (65 wt%) without the contribution of conductive and binder additives is considered.

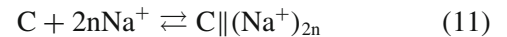
Returning to figure 6(a), a sharp increase of current is observed in the I, II and III, IV potential regions indicating the beginning of harmful faradaic processes of H₂ and O₂ evolution, respectively. Therefore, the negative or positive polarization of the electrodes over these potentials for a long time should be avoided, because pH of the near-electrode solution is shifted from neutral to more alkaline/acidic range that may adversely affect the stability of the Ag/Ag₂SO₄ RE situated close to the surface of the working electrode.

The values of capacitance normalized per mass of the working electrode (*i.e.*, specific capacitance C_{sp}) and operating potential ranges for the carbon-based electrodes are collected in table 2. Using them in Eq. 2, we get the mass ratio of the negative and positive electrodes as 1.1, and the cyclic voltammogram of this mass-balanced two-electrode cell is shown in figure 6(b) (its characteristics are also presented in table 2). As shown, it operates at the voltage, which is 500 mV higher than the potential range where water is electrochemically stable.

Based on the charge storage mechanism for electric double layer capacitor-type and battery-type materials proposed in Refs.,^{30–33} one can write the reaction which occurs during the charge-discharge of the positively hybridized carbon nanotube/MnO₂ electrode as follows:



where M⁺ are the alkali metal cations (K⁺ from KMnO₄ used for synthesis of the carbon nanotube/MnO₂ composite and Na⁺ as a cation part of the electrolyte solution); || represents the electric-double layer. The charge storage mechanism on the positive electrode is a complex process combining the intercalation–deintercalation of alkali metal ion in manganese dioxide and the sorption–desorption of sulfate anions in carbon nanotube matrix. As for the negative graphene electrode, the charge–discharge of the electric-double layer takes place as follows:



Analyzing data from table 2 and figure 6(b), one observes at least 4-fold reduction in specific capacitance of the supercapacitor cell compared to the single electrodes. This is quite predictable and, moreover, confirms the correctness of the mass balancing procedure described by Khomenko *et al.*¹⁴ The total capacitance of the supercapacitor C_{cell} depends on capacitances of each electrode and is expressed by the following equation:

$$\frac{1}{C_{cell}} = \frac{1}{C_1} + \frac{1}{C_2} \quad (12)$$

There are two different cases to be considered: (i) if the capacitances of both electrodes are equal ($C_1 = C_2$), the cell capacitance is,

$$C_{cell} = \frac{C_1}{2} \quad (13)$$

(ii) if capacitances of the negative and positive electrodes differ too much (*e.g.*, $C_1 \ll C_2$), the capacitance of the supercapacitor cell is limited by the lower capacitance value and Equation transforms to

$$C_{\text{cell}} \approx C_1 \quad (14)$$

i.e., C_{cell} varies in the $\left(\frac{C_1}{2} \dots C_1\right)$ range and $C_{\text{cell}} \rightarrow C_1$ if the difference between capacitances of the single electrodes increases.

In our case, the electrodes are of almost similar specific capacitances ($C_{1\text{-sp}} \approx C_{2\text{-sp}}$) and Eq. 1 gives the mass balancing ratio as 1.1; therefore the specific cell capacitance $C_{\text{cell-sp}}$ should be approx. 4 times lower than capacitances of electrode:

$$C_{\text{cell-sp}} \approx \frac{C_1}{2 \times 2m_1} \approx \frac{C_{1\text{-sp}}}{4} \quad (15)$$

This means that the specific capacitance of the graphene-carbon nanotube/MnO₂ supercapacitor must be 22 F g⁻¹ according to Eq. 15, but this electrochemical system demonstrates a little bit higher value due to the assumptions made (equality of the electrode masses and their specific capacitances). The use of the symmetrical (mass-unbalanced) systems leads to a sharp drop in capacitance at the transition from a three-electrode cell to the 'real' two-electrode device due to the different amount of charge accumulated per single electrode during working of a supercapacitor, as shown in Ref.³⁴

Taking into account the values of the specific capacitance and operating voltage defined from figure 6(b) (23 F g⁻¹ and 1.75 V), the specific energy E of the graphene-carbon nanotube/MnO₂ supercapacitor measured in Watt·hour per kilogram of both electrodes may be calculated through the equation:

$$E = \frac{C_{\text{cell-sp}} U^2}{2 \times 3.6} \quad (16)$$

In order to compare the specific energy obtained by means of Equation 16 (9.8 Wh kg⁻¹) with specific energies of commercial ultracapacitors, which are related to the mass of the whole device including masses of the electrolyte, metallic current collectors, case, *etc.*, this value needs to be multiplied by a correction factor. Du Pasquier *et al.*,³⁵ estimated that the contribution of the electrodes into the total mass of a flat supercapacitor cell assembled in a soft case is about 35%. Consequently, the specific energy of the supercapacitor based on graphene and carbon nanotube/MnO₂ electrodes built in this study should be reduced to 3.4 Wh kg⁻¹, while commercial devices from the market leaders (*viz.*, Maxwell, NessCap) working with electrolytes containing aprotic nonaqueous solvents have the specific energy ranging from 3.2 to 6.0 Wh kg⁻¹.³⁶

4. Conclusions

In this paper, the possibility to use the Ag/Ag₂SO₄ system as a planar RE for *in-situ* electrochemical studies of the supercapacitor electrodes in neutral aqueous solutions has been demonstrated. The key characteristics of this RE made *via* a simple and rapid chemical technique have been determined: its position between other commonly used REs (*viz.*, +0.137 V vs. Ag/AgCl), its temperature coefficient depending on concentration of the potential-determining ions (*ca.* -0.7 mV °C⁻¹), potential drift (0.1 mV h⁻¹), and potential deviations (±0.5 mV).

Furthermore, the constant potential of the SSE in different supporting solutions (alkali metal sulphates, nitrates and chlorides) has been demonstrated and a number of 'undesirable' electrolytes (strong acids and bases) for long-time usage have been defined.

On the basis of the electrochemical measurements in the three-electrode cell of flat design with the prepared Ag/Ag₂SO₄ RE, an environmentally friendly advanced graphene-carbon nanotube/MnO₂ supercapacitor with Na₂SO₄-H₂O solution operating at the extended voltage (1.75 V) has been assembled. The expected value of energy (normalized per mass of the whole cell) for such device is comparable to specific energies of commercial supercapacitors with nonaqueous organic electrolytes, despite more than 1.5-fold difference in their rated voltages.

Acknowledgements

The author thanks to Dr. S.A. Kirillov for his valuable advice in writing this work.

References

1. Maletin Y, Strelko V, Stryzhakova N, Zelinsky S, Rozhenko A B, Gromadsky D, Volkov V, Tychina S, Gozhenko O and Drobny D 2013 *Energy Environ. Res.* **3** 156
2. Ribeiro P F, Johnson B K, Crow M L, Arsoy A and Liu Y 2001 *Proc. IEEE* **12** 1744
3. Chu A and Braatz P 2002 *J. Power Sources* **112** 236
4. Wang G, Zhang L and Jang J 2012 *Chem. Soc. Rev.* **41** 797
5. Stevenson A J, Gromadskyi D G, Hu D, Chae J, Guan L, Yu L and Chen G Z 2015 In *Nanocarbons for Advanced Energy Storage* X Feng (Ed.) (Weinheim: Wiley-VCH)
6. Wang F, Xiao S, Hou Y, Hu C, Liu L and Wu Y 2013 *RSC Adv.* **3** 13059
7. Liu B, Wang X, Chen D, Fan Z and Shen G 2014 *Nano Energy* **10** 99
8. Masarapu C, Wang L P, Li X and Wei B 2012 *Adv. Energy Mater.* **2** 546
9. Liivand K, Thomberg T, Jänes A and Lust E 2015 *ECS Trans.* **64** 41

10. Zhong C, Deng Y, Hu W, Qiao J, Zhang L and Zhang J 2015 *Chem. Soc. Rev.* **44** 7484, DOI: [10.1039/C5CS00303B](https://doi.org/10.1039/C5CS00303B)
11. Hromadský D H, Fateev Y F, Stryzhakova N H and Maletin Y A 2010 *Mater. Sci.* **46** 412
12. Gromadskyi D G, Fateev Y F and Maletin Y M 2013 *Corros. Sci.* **69** 191
13. Zhao F, Wang Y, Xu X, Liu Y, Song R, Lu G and Li Y 2014 *ACS Appl. Mater. Interfaces* **6** 11007
14. Khomenko V, Raymundo-Piñero E and Béguin F 2006 *J. Power Sources* **153** 183
15. Gromadskyi D G, Chae J H, Norman S A and Chen G Z 2015 *Appl. Energy* **159** 39
16. Bott A W 1995 *Curr. Sep.* **14** 64
17. Bard A J, Parsons R and Jordan J 1985 In *Standard Potentials in Aqueous Solutions* (New York: Marcel Dekker)
18. Hamer W J and Wu Y C 1995 *J. Solution Chem.* **24** 1013
19. Velický M, Tam K Y and Dryfe R A W 2012 *Anal. Methods* **4** 1207
20. Ruetschi P 2003 *J. Power Sources* **113** 363
21. https://www.basinc.com/mans/EC_epsilon/Techniques/CPot/ocp.html. Accessed on 09.12.2015
22. Subramanian V, Zhu H and Wei B 2006 *Electrochem. Commun.* **8** 827
23. Shaffer M S P, Fan X and Windle A H 1998 *Carbon* **36** 1603
24. Hoshi Y, Narita Y, Honda K, Ohtaki T, Shitanda I and Itagaki M 2015 *J. Power Sources* **288** 168
25. Cimenti M, Co A C, Birss V I and Hill J M 2007 *Fuel Cells* **7** 364
26. Wang H, Forse A C, Griffin J M, Trease N M, Trognko L, Taberna P L, Simon P and Grey C P 2013 *J. Am. Chem. Soc.* **135** 18968
27. Sawuyer D T, Sobkowiak A and Roberts J L 1995 In *Electrochemistry for Chemists* (New York: Wiley)
28. Shiue M Y, Sun Y C, Yeh J J, Yang J Y and Yang M H 1999 *Analyst* **124** 15
29. Ghodbane O, Pascal J L and Favier F 2009 *ACS Appl. Mater. Interfaces* **1** 1130
30. Toupin M, Brousse T and Bélanger D 2004 *Chem. Mater.* **16** 3184
31. Simon P and Gogotsi Y 2008 *Nat. Mater.* **7** 845
32. Hsieh C T and Teng H 2002 *Carbon* **40** 667
33. Khomenko V, Frackowiak E and Béguin F 2005 *Electrochim. Acta* **50** 2499
34. Stoller M D and Ruoff R S 2010 *Energy Environ. Sci.* **3** 1294
35. Du Paquier A, Shelburne J A, Plitz I, Badway F, Gozdz A S, Amatucci G G 2001 In *Proc. 11th Int. Semin. Double Layer Capacitors Similar Energy Storage Devices*, (Deerfield Beach, FL, USA: Florida Educational Seminars Inc.)
36. Zhang J and Zhao X S 2012 *Chem. Sus. Chem.* **5**(2012) 818